

Fundamental Limits for Jammer-Resilient Communication in Finite-Resolution MIMO

Gian Marti, Alexander Stutz-Tirri, and Christoph Studer

Department of Information Technology and Electrical Engineering, ETH Zurich, Switzerland

email: gimarti@ethz.ch, alstutz@iis.ee.ethz.ch, and studer@ethz.ch

Abstract—Spatial filtering based on multiple-input multiple-output (MIMO) processing is a powerful method for jammer mitigation. In principle, a MIMO receiver can null the interference of a single-antenna jammer at the cost of only one degree of freedom—if the number of receive antennas is large, communication performance is barely affected. In this paper, we show that the potential for MIMO jammer mitigation based on the digital outputs of finite-resolution analog-to-digital converters (ADCs) is fundamentally worse: Strong jammers will either cause the ADCs to saturate (when the ADCs’ quantization range is small) or drown legitimate communication signals in quantization noise (when the ADCs’ quantization range is large). We provide a fundamental bound on the mutual information between the quantized receive signal and the legitimate transmit signal. Our bound shows that, for any fixed ADC resolution, the mutual information tends to zero as the jammer power tends to infinity, regardless of the quantization strategy. Our bound also confirms the intuition that for every 6.02 dB increase in jamming power, the ADC resolution must be increased by 1 bit in order to prevent the mutual information from vanishing.

I. INTRODUCTION

Jammers are natural enemies of wireless communication systems [1]. A powerful countermeasure is spatial filtering via multiple-input multiple-output (MIMO) processing [2], [3]. If the receive signal at a B -antenna receiver consists of the linear superposition of legitimate communication signals and low-rank jammer interference, then the receiver can null the jammer interference at the cost of I degrees of freedom (where I is the rank of the jammer interference). If $B \gg I$ and the wireless channel is well conditioned, then communication performance is barely affected by the jammer. However, if the receive signal is converted to digital using analog-to-digital converters (ADCs) before equalization, then the relation between the transmit signals and the finite-resolution digital receive signals is no longer linear [4]–[6]. In particular, strong jammers cause the ADCs to saturate when the ADCs’ quantization range is small, and they drown legitimate communication signals in quantization noise when the ADCs’ quantization range is large [7].

A. Contributions

We show that quantization *fundamentally* limits jammer-resilient communication in MIMO systems. To this end, we derive a bound on the mutual information between the quantized receive signal and the legitimate transmit signal as a function of the ADC resolution and the receive signal-to-interference-plus-noise ratio (SINR). Our bound holds for *any* ADCs with a given resolution (not only for uniform quantizers, and regardless of what kind of automatic gain control is applied) and for *any* power-limited signaling at the legitimate transmitters (not only

for QAM or Gaussian signals). Our bound reveals that, for any fixed ADC resolution, the mutual information tends to zero as the jammer power tends to infinity. Furthermore, our results rigorously confirm the intuition that the ADC resolution must be increased by 1 bit for every 6.02 dB increase in jamming power to prevent the mutual information from vanishing. We complete our analysis with numerical simulations and with a comparison to the behavior of infinite-resolution MIMO communication systems (which are analyzed in App. A).

B. Notation

Matrices, vectors, and scalars are denoted by boldface uppercase (e.g., \mathbf{A}), boldface lowercase (e.g., \mathbf{a}), and italic or sans-serif (e.g., a , A , and A), respectively. For a matrix \mathbf{A} , the transpose is \mathbf{A}^T , the (entry-wise) conjugate is \mathbf{A}^* , the conjugate transpose is \mathbf{A}^H , the determinant is $|\mathbf{A}|$, the space spanned by its columns is $\text{col}(\mathbf{A})$, and the n th row is $\mathbf{a}_{(n)}$. The Euclidean norm is $\|\cdot\|_2$. A circularly-symmetric complex Gaussian vector with covariance matrix \mathbf{C} is denoted $\mathbf{a} \sim \mathcal{CN}(\mathbf{0}, \mathbf{C})$. Whether a quantity is a random variable or a constant becomes clear from the context. Mutual information, conditional mutual information, discrete entropy, conditional discrete entropy, differential entropy, and conditional differential entropy are denoted by $I(\cdot; \cdot)$, $I(\cdot; \cdot | \cdot)$, $H(\cdot)$, $H(\cdot | \cdot)$, $h(\cdot)$, and $h(\cdot | \cdot)$, respectively. Logarithms are to the basis 2. The binary entropy function is $H_b(x) = -x \log(x) - (1-x) \log(1-x)$ and we use $\bar{H}_b(x) = H_b(\min\{x, \frac{1}{2}\})$. The (complementary) error function is $\text{erf}(x) = 2\pi^{-1/2} \int_0^x \exp(-t^2) dt$ and $\text{erfc}(x) = 1 - \text{erf}(x)$, respectively. $[N]$ is the set of integers from 1 through N and $\lfloor x \rfloor$ is the largest integer no greater than x . $\mathbb{1}\{\text{statement}\}$ equals 1 if statement is true and 0 otherwise. For the functions f and g , the relation $f \prec g$ means that $\exists \epsilon > 0 : \lim_{x \rightarrow \infty} \frac{f(x)}{g(x)} x^\epsilon = 0$, and $f \succeq g$ is its logical negation. The relation $f \prec_+ g$ means that $\exists \epsilon > 0 : \lim_{x \rightarrow \infty} (1 + \epsilon)f(x) - g(x) = -\infty$, and $f \succeq_+ g$ is its logical negation. We use $\inf_{\mathcal{A}} f$ as shorthand for $\inf_{x \in \mathcal{A}} f(x)$.

II. SYSTEM MODEL

We consider a frequency-flat MIMO system under jamming. We focus on a multi-user (MU) MIMO uplink scenario, but our results are easily extended to single-input multiple-output or point-to-point MIMO scenarios. We model the time-sampled receive signal $\mathbf{y} \in \mathbb{C}^B$ at a B -antenna basestation (BS) as

$$\mathbf{y} = \mathbf{H}\mathbf{s} + \mathbf{J}\mathbf{w} + \mathbf{n}, \quad (1)$$

where $\mathbf{H} \in \mathbb{C}^{B \times U}$ is the channel matrix of U legitimate single-antenna user equipments (UEs) with data signal $\mathbf{s} \in \mathbb{C}^U$, $\mathbf{J} \in \mathbb{C}^{B \times I}$ is the channel matrix of an I -antenna jammer with

transmit vector $\mathbf{w}_k \in \mathbb{C}^I$, and $\mathbf{n} \sim \mathcal{CN}(\mathbf{0}, N_0 \mathbf{I}_B)$ is circularly-symmetric complex white Gaussian noise. We assume that the matrices \mathbf{H} and \mathbf{J} stay constant over an extended time period (slow fading) and are perfectly known at the receiver.¹ The random vectors \mathbf{s} , \mathbf{w} , and \mathbf{n} are assumed to be mutually independent. By defining the receive data signal $\mathbf{r} \triangleq \mathbf{H}\mathbf{s}$ and the receive interference $\mathbf{z} \triangleq \mathbf{J}\mathbf{w}$, we can rewrite (1) as

$$\mathbf{y} = \mathbf{r} + \mathbf{z} + \mathbf{n}. \quad (2)$$

We then model analog-to-digital conversion at the BS by quantizing the time-sampled receive signal \mathbf{y} in amplitude using

$$\mathbf{q} = \mathcal{Q}(\mathbf{y}), \quad (3)$$

where

$$\mathcal{Q} : \mathbb{C}^B \rightarrow \mathcal{Q}^{2B}, \quad \mathbf{y} \mapsto (q_{(1,\tau)}, q_{(1,i)}, \dots, q_{(B,\tau)}, q_{(B,i)}) \quad (4)$$

$$q_c = Q_c(y_c), \quad c \in \mathcal{C} \triangleq [B] \times \{\tau, i\}, \quad (5)$$

quantizes the in-phase and quadrature parts (indexed by τ and i , respectively) of the receive signal \mathbf{y} using scalar quantizers $Q_c : \mathbb{R} \rightarrow \mathcal{Q}_c$ with $M \triangleq |\mathcal{Q}_c| \geq 2$ quantization levels. The scalar quantizers Q_c may be non-uniform and different for every $c \in \mathcal{C}$, but we assume that the ADC resolution M is the same for all $c \in \mathcal{C}$. Equations (2) and (3) can be restated for the scalar signal components $c \in \mathcal{C}$ as

$$y_c = r_c + z_c + n_c \quad (6)$$

$$q_c = Q_c(y_c). \quad (7)$$

III. MAIN RESULT

We state our main result in three steps; all proofs are in App. B. First, we relate the mutual information between \mathbf{q} and \mathbf{s} to the sum over conditional mutual informations between the signal components r_c and the ADC outputs q_c , given the interference-plus-noise components $z_c + n_c$:

Theorem 1. Consider the model from Sec. II. Then

$$I(\mathbf{q}; \mathbf{s}) \leq \min \left\{ \sum_{c \in \mathcal{C}} I(q_c; r_c | z_c + n_c), \log |N_0^{-1} \mathbf{H}\mathbf{H}^H + \mathbf{I}_B| \right\}. \quad (8)$$

(The second argument in the minimum comes from the fact that the mutual information is always bounded by the capacity of an unquantized, jammer-free system; cf. App. A.) Second, we bound the conditional mutual information in (8) in terms of the number of quantization levels and the SINR:

Theorem 2. Consider the model from Sec. II for $z_c \sim \mathcal{N}(0, Z_c)$, $n_c \sim \mathcal{N}(0, N_0)$, and $\mathbb{E}[|r_c|^2] \leq R_c$. Let

$$\text{SINR}_c \triangleq \frac{R_c}{Z_c + N_0} \quad (9)$$

denote the SINR at the c th ADC and define

$$\bar{f}(M, \text{SINR}_c) = \text{erf} \left(\frac{(M-1)\sqrt{\text{SINR}_c}}{\sqrt{2}} \right)$$

¹The assumption of perfect channel knowledge strengthens our result: An upper bound on possible rates of communication with perfect channel knowledge also holds when the channels are not known, or known imperfectly.

$$+ \sqrt{\frac{2}{\pi}} (M-1) \sqrt{\text{SINR}_c} \exp \left(-\frac{(M-1)^2 \text{SINR}_c}{2} \right) - (M-1)^2 \text{SINR}_c \text{erfc} \left(\frac{(M-1)\sqrt{\text{SINR}_c}}{\sqrt{2}} \right) \quad (10)$$

and

$$\bar{l}(M, \text{SINR}_c) \triangleq \min \left\{ \log M, \bar{H}_b(\bar{f}(M, \text{SINR}_c)) + \bar{f}(M, \text{SINR}_c) \log(M-1) \right\}. \quad (11)$$

Then, the conditional mutual information $I(q_c, r_c | z_c + n_c)$ is bounded by

$$I(q_c; r_c | z_c + n_c) \leq \bar{l}(M, \text{SINR}_c). \quad (12)$$

Remark 1. The statement of Thm. 2 also holds when, in (11), $\bar{f}(M, \text{SINR}_c)$ is replaced with its upper bound

$$\bar{\bar{f}}(M, \text{SINR}_c) = \sqrt{\frac{8}{\pi}} (M-1) \sqrt{\text{SINR}_c}. \quad (13)$$

A derivation of this upper bound is shown in App. B-E.

The final step combines the results from Thm. 1 and Thm. 2:

Theorem 3. Consider the model from Sec. II, and assume that $\mathbf{w} \sim \mathcal{CN}(\mathbf{0}, \rho \mathbf{I}_I)$, that $\mathbf{n} \sim \mathcal{CN}(\mathbf{0}, N_0 \mathbf{I}_B)$, and that the entries s_u of \mathbf{s} are uncorrelated and satisfy $\mathbb{E}[|s_u|^2] \leq 1$. Then

$$I(\mathbf{q}; \mathbf{s}) \leq \bar{I}(M, \rho, \mathbf{H}, \mathbf{J}) \quad (14)$$

$$\triangleq \min \left\{ \sum_{c \in \mathcal{C}} \bar{l}(M, \overline{\text{SINR}}_c), \log |N_0^{-1} \mathbf{H}\mathbf{H}^H + \mathbf{I}_B| \right\}, \quad (15)$$

where $\overline{\text{SINR}}_c \geq \text{SINR}_c$ is an upper bound on the SINR at the c th ADC which, for $c \in \{(b, \tau), (b, i)\}$, is given by

$$\overline{\text{SINR}}_c = \frac{2 \|\mathbf{h}_{(b)}\|_2^2}{\rho \|\mathbf{j}_{(b)}\|_2^2 + N_0}. \quad (16)$$

Remark 2. If $\mathbf{s} \sim \mathcal{CN}(\mathbf{0}, \mathbf{I}_U)$, then (16) can be tightened to

$$\text{SINR}_c = \overline{\text{SINR}}_c = \frac{\|\mathbf{h}_{(u)}\|_2^2}{\rho \|\mathbf{j}_{(u)}\|_2^2 + N_0}. \quad (17)$$

IV. ANALYSIS

A. Asymptotic Analysis

For fixed channel realizations \mathbf{H} and \mathbf{J} , and for a fixed thermal noise power N_0 , the bound in (14) is a function of the jammer power ρ (via (16)) and the number of ADC quantization levels M . Two questions are therefore natural to ask:²

- 1) What happens in the limit $\rho \rightarrow \infty$ when the ADC resolution M is fixed?
- 2) How does the ADC resolution M have to scale with ρ to prevent the mutual information $I(\mathbf{q}; \mathbf{s})$ from vanishing?

The answers to these questions are as follows:

Proposition 1. Consider the model from Sec. II, and assume that $\mathbf{w} \sim \mathcal{CN}(\mathbf{0}, \rho \mathbf{I}_I)$, $\mathbf{n} \sim \mathcal{CN}(\mathbf{0}, N_0 \mathbf{I}_B)$, and that the entries s_u of \mathbf{s} are uncorrelated and satisfy $\mathbb{E}[|s_u|^2] \leq 1$. If all rows of \mathbf{J} are nonzero, then $I(\mathbf{q}; \mathbf{s}) \xrightarrow{\rho \rightarrow \infty} 0$.

²The attentive reader will notice that the second question presupposes the answer to the first question.

Proposition 2. Consider the model from Sec. II, and assume that $\mathbf{w} \sim \mathcal{CN}(\mathbf{0}, \rho \mathbf{I}_I)$, that $\mathbf{n} \sim \mathcal{CN}(\mathbf{0}, N_0 \mathbf{I}_B)$, and that the entries s_u of \mathbf{s} are uncorrelated and satisfy $\mathbb{E}[|s_u|^2] \leq 1$. If all rows of \mathbf{J} are nonzero, then $\lim_{\rho \rightarrow \infty} I(\mathbf{q}; \mathbf{s}) > 0$ implies

$$M \succeq \sqrt{\rho}. \quad (18)$$

Equation (18) can be restated in the logarithmic domain as

$$\log M \succeq_+ \frac{\log 10}{20} \rho_{\text{dB}} \approx \frac{1}{6.02} \rho_{\text{dB}}, \quad (19)$$

which implies that one additional bit of ADC resolution is needed for every 6.02 dB increase in jammer power!

B. Numerical Analysis

We turn to the numerical analysis of our results. We start by plotting the bound $\bar{v}(M, \text{SINR}_c)$ from Thm. 2 as a function of the reciprocal signal-to-interference-plus-noise ratio SINR_c^{-1} , for different numbers of quantization levels M (note that the number of quantization levels for an m -bit quantizer is $M = 2^m$). Fig. 1 depicts the bounds $\bar{v}(M, \text{SINR}_c)$ from Thm. 2 (solid lines) as well as the (slightly) looser bounds based on the easier-to-interpret function $\bar{f}(M, \text{SINR}_c)$ from Rem. 1 (dashed lines). For any fixed ADC resolution, Fig. 1 shows the following: The conditional (on the interference plus noise) entropy of an ADC output is guaranteed to be strictly smaller than its number of output bits when the SINR_c^{-1} at that ADC's input exceeds a certain value; and the conditional mutual information tends to zero with increasing SINR_c^{-1} . An ADC with a large SINR_c^{-1} at its input will therefore barely contribute to the mutual information $I(\mathbf{q}; \mathbf{s})$; cf. Thm. 3.

Fig. 1 also exemplarily marks (in gray) the SINR_c^{-1} levels at which the conditional mutual information of an ADC falls below 2 bits: If SINR_c^{-1} exceeds 74.0 dB, then the conditional entropy of a 9-bit quantizer is smaller than 2 bits; if SINR_c^{-1} exceeds 80.8 dB, then the conditional entropy of a 10-bit quantizer is smaller than 2 bits. These results point towards the result from Prop. 2: Asymptotically, the ADC resolution must increase by one bit for every 6.02 dB of increased jamming power to prevent its conditional mutual information (and thus the overall mutual information; cf. Thm. 1) from vanishing.

Next, we evaluate the bound on $I(\mathbf{q}; \mathbf{s})$ from Thm. 3 as a function of the channel realizations \mathbf{H} and \mathbf{J} . To this end, we consider a MU-MIMO system with $B = 16$ receive antennas (corresponding to $|\mathcal{C}| = 32$ receive ADCs), $U = 2$ UEs, and an $I = 1$ antenna jammer that transmits Gaussian symbols with $\rho = 60$ dB more power than each of the UEs. The signal-to-noise ratio (SNR) is assumed to be 30 dB (i.e., we have $N_0 = -30$ dB, meaning that the noise on its own plays no significant role). We consider two different channel models: (i) Rayleigh fading, where the entries of \mathbf{H} and \mathbf{J} are drawn i.i.d. according to $\mathcal{CN}(0, 1)$; and (ii) a textbook line-of-sight (LoS) model in which the BS antennas are arranged in a uniform linear array (ULA) with half-wavelength antenna spacing and where the UEs and the jammer are placed uniformly independently in a 120° sector in front of the BS, so that the channel vector between the BS and a device placed at angle θ is

$$[1, e^{-i\pi \cos(\theta)}, \dots, e^{-i\pi \cos(\theta)(B-1)}]^T. \quad (20)$$

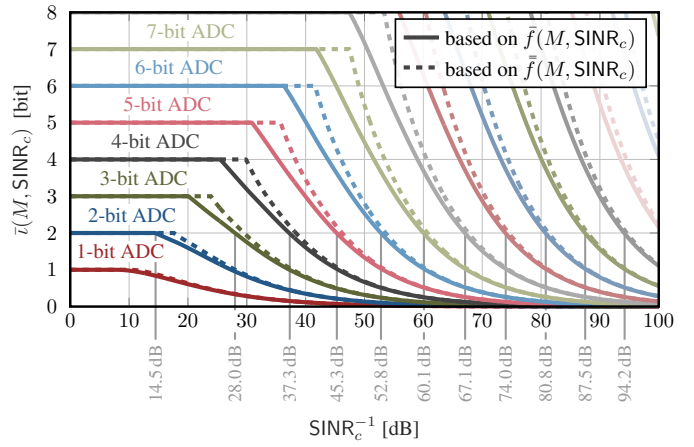


Fig. 1. The bound from Thm. 2 as a function of the reciprocal signal-to-interference-plus-noise ratio SINR_c^{-1} . The number M of ADC quantization levels is expressed by the number of equivalent bits $\log M$. Dashed curves are based on the weaker (but more intuitive) bound from Rem. 1.

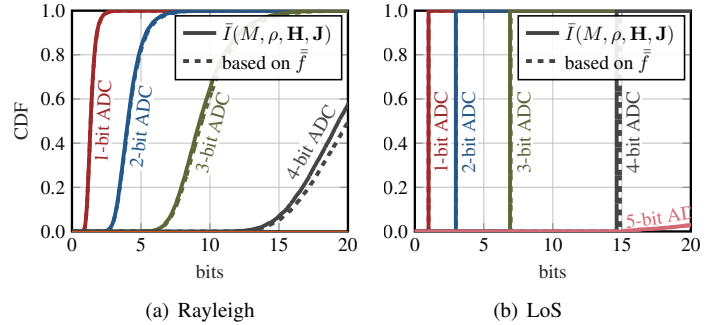


Fig. 2. Cumulative distribution functions (CDFs) over channel realizations of the bound from Thm. 3, for two different channel models. The number M of ADC quantization levels is expressed by the number of equivalent bits $\log M$. Dashed curves are based on the weaker bound from Rem. 1.

Note that we do not model path loss explicitly in either the Rayleigh fading or the LoS model: Differences in path loss between the UEs are assumed to be compensated by UE power control, and differences in path loss between the UEs and the jammer are absorbed into the jammer transmit power ρ .

In Fig. 2, we plot the cumulative distribution function (CDF) of $\bar{I}(M, \rho, \mathbf{H}, \mathbf{J})$ over random channel realizations. Fig. 2(a) shows that, for 90% of Rayleigh fading channel realizations, the mutual information $I(\mathbf{q}; \mathbf{s})$ under 1-bit quantization is lower than 2 bits. In these cases, the jammer can reduce the mutual information between the quantized receive signal and the data signal by more than $30/32 = 93.75\%$ (because the $|\mathcal{C}| = 32$ 1-bit ADCs in principle have the potential to deliver 32 bits of information about \mathbf{s}).³ Hence, for these channel realizations, the possible rates of communication are reduced by more than 93.75% compared to a jammer-free scenario *regardless* of any potential jammer-mitigating equalization, linear or non-linear, that is applied to the digital signal \mathbf{q} . This behavior contrasts sharply with the jammer resilience of infinite-resolution MIMO

³In this argument, we assume that the thermal noise plays essentially no role here in reducing the mutual information. This assumption is validated by the fact that the CDFs from Fig. 2 are virtually identical when the noise \mathbf{n} is set to zero—the noise \mathbf{n} contributes virtually nothing to the SINRs underlying the CDFs from Fig. 2 since it has orders of magnitude less energy than \mathbf{w} .

communication systems with $\mathbf{q} = \mathbf{y}$, for which lower bounds on $I(\mathbf{y}; \mathbf{s})$ can be obtained that are independent of the jammer power, and that are close to the mutual information of equivalent jammer-free systems; see App. A for the details.

Fig. 2(b) shows results for LoS channels, which are qualitatively similar the results of Fig. 2(a). However, for the textbook LoS model in (20), the norms of rows of the channel matrices \mathbf{H} and \mathbf{J} are deterministic, $\|\mathbf{h}_{(b)}\|_2^2 = U$, and $\|\mathbf{j}_{(b)}\|_2^2 = I$. As a result, $\bar{I}(M, \rho, \mathbf{H}, \mathbf{J})$ in (14) becomes deterministic and the CDFs turn into step-functions that depend only on M and ρ (provided that the second argument of the minimum in (15) is not smaller than the first one; see the 5-bit ADC in Fig. 2(b)). Fig. 2(b) shows that the mutual information $I(\mathbf{q}; \mathbf{s})$ is lower than 1 bit when 1-bit quantizers are used, and lower than 3 bits when 2-bit quantizers are used.

V. RELATED WORK

Jamming attacks on MIMO communication systems and finite- or low-resolution MIMO systems have independently been studied, e.g., in [1], [3], [8] and [4], [5], [9] as well as the references therein, but the interplay of these two phenomena has received comparably less attention. The first work that studies the interplay between jamming and finite-resolution quantization is [7], which analyzes the impact of out-of-band jammers on single-input single-output (SISO) communication systems with uniform quantizers. For such systems, and based on heuristic arguments, [7] suggests a similar criterion to the one in Prop. 2 for successful communication. The fact that jammer-resilient data detectors require higher resolution than non-resilient ones has also been observed empirically in [10]. Reference [11] considers the effect of ADC quantization noise due to jamming in the context of global navigation satellite systems (GNSSs) and suggests oversampling as a remedy.

More recently, a number of papers have considered the adverse impact of strong jamming on low-resolution MIMO communication systems and proposed various ways of removing a significant part of the jammer interference *before* it is quantized by the ADCs [12]–[15]. Reference [12] proposes the use of spatial sigma-delta converters to form a spatial filter that removes the jammer interference in the analog domain. Reference [13] suggests to use a hybrid scheme consisting of an adaptive analog transform, which removes most of the jammer energy before it reaches the ADCs, and a subsequent digital equalizer that suppresses potential residues. For communication at millimeter-wave (mmWave) frequencies, [14] proposes a non-adaptive analog transform that sparsifies mmWave wireless channels and thus focuses the jammer interference on a subset of ADCs, so that the data signals can be reconstructed based on the outputs of the interference-free ADCs. Reference [15] suggests the use of a reconfigurable intelligent surface (RIS) to steer jamming signals away from the ADCs.

Finally, [16] proposes a method for detecting jammers in MIMO systems with 1-bit quantizers, but does not consider methods for their subsequent mitigation.

VI. CONCLUSIONS

We have derived fundamental information-theoretic limits for communication in finite-resolution MIMO under jamming.

Our results have shown that, for any fixed ADC resolution, the mutual information between the legitimate communication signals and the quantized receive signal tends to zero as the jammer power tends to infinity. This shows that finite-resolution MIMO systems are fundamentally vulnerable to jamming attacks in a way that infinite-resolution systems are not. In consequence, it is beneficial to mitigate jammers already *before* data conversion, e.g., using the methods proposed in [13], [14].

APPENDIX A RESULTS ON THE JAMMER-RESILIENCE OF INFINITE-RESOLUTION MIMO

Prop. 1 from Sec. IV demonstrates that a single-antenna jammer can drive the rates at which data transmission to a low-resolution multi-antenna BS is possible to zero, regardless of any jammer-mitigating equalization that might be applied to the digital receive signal. Moreover, the results from Sec. IV-B show that a 60 dB single-antenna jammer can reduce the rates at which communication from $U = 2$ UEs to a $B = 16$ antenna BS with 1-bit ADCs is possible by more than 93.75% compared to a jammer-free scenario.

We now show that *infinite-resolution* MIMO communication systems do not share such a vulnerability against single- or few-antenna jammers, provided that the spatial diversity is sufficient. For this, we consider a communication system as in Sec. II—except that, since the receiver is assumed to be infinite-resolution, we focus on the mutual information $I(\mathbf{y}; \mathbf{s})$ between \mathbf{s} and the *unquantized* receive signal \mathbf{y} . Our analysis will make use of the projection onto the orthogonal complement of the jammer subspace, given by the matrix \mathbf{U}_\perp^H , whose rows form an orthonormal basis of the orthogonal complement of $\text{col}(\mathbf{J})$.⁴ This operator can be used as a spatial filter at the BS and has the property that $\mathbf{U}_\perp^H \mathbf{J} = \mathbf{0}$. Since all channels are known, the BS knows \mathbf{U}_\perp^H . We then have the following results:

Proposition 3. *Consider the input-output relation in (1), and assume that $\mathbf{s} \sim \mathcal{CN}(\mathbf{0}, \mathbf{I}_U)$ and $\mathbf{n} \sim \mathcal{CN}(\mathbf{0}, N_0 \mathbf{I}_B)$. The distribution of the jammer signal \mathbf{w} can be arbitrary. Then, for every fixed realization of \mathbf{H} and \mathbf{J} ,*

$$I(\mathbf{y}; \mathbf{s}) \geq \underline{I}(\mathbf{H}, \mathbf{J}) \triangleq \log |N_0^{-1} \mathbf{U}_\perp^H \mathbf{H} \mathbf{H}^H \mathbf{U}_\perp + \mathbf{I}_{B-I}|. \quad (21)$$

Proposition 4. *Consider the input-output relation in (1). If $\mathbf{n} \sim \mathcal{CN}(\mathbf{0}, N_0 \mathbf{I}_B)$ is white Gaussian noise and $\mathbf{H} \in \mathbb{C}^{B \times U}$ and $\mathbf{J} \in \mathbb{C}^{B \times I}$ are Rayleigh fading channels, $\mathbf{H} \stackrel{\text{i.i.d.}}{\sim} \mathcal{CN}(0, 1)$, $\mathbf{J} \stackrel{\text{i.i.d.}}{\sim} \mathcal{CN}(0, 1)$, then the filtered input-output relation*

$$\mathbf{U}_\perp^H \mathbf{y} = \mathbf{U}_\perp^H (\mathbf{H} \mathbf{s} + \mathbf{J} \mathbf{w} + \mathbf{n}) \quad (22)$$

is equivalent to

$$\tilde{\mathbf{y}} = \tilde{\mathbf{H}} \mathbf{s} + \tilde{\mathbf{n}}, \quad (23)$$

where $\tilde{\mathbf{H}} \in \mathbb{C}^{(B-I) \times U}$ is Rayleigh fading, $\tilde{\mathbf{H}} \stackrel{\text{i.i.d.}}{\sim} \mathcal{CN}(0, 1)$, and $\tilde{\mathbf{n}} \sim \mathcal{CN}(\mathbf{0}, N_0 \mathbf{I}_{B-I})$ is white Gaussian noise. In other words, any impact of the jammer can be mitigated via spatial filtering by sacrificing the equivalent of I antennas at the BS.

⁴Strictly speaking, \mathbf{U}_\perp^H is not a projection—only $\mathbf{U}_\perp \mathbf{U}_\perp^H$ is. We refer to \mathbf{U}_\perp^H as a projection nonetheless.

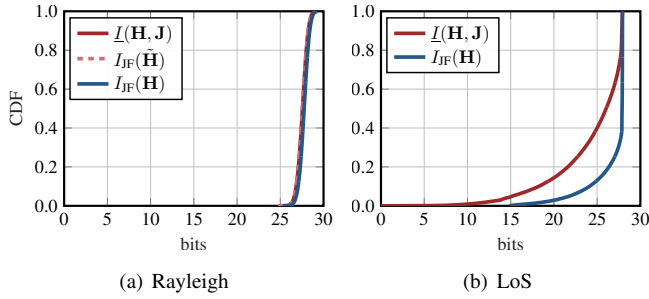


Fig. 3. Cumulative distribution functions (CDFs) over channel realizations of the lower bound from Prop. 3 and of the jammer-free mutual information from (24) for two different channel models. Fig. 3(a) also plots the CDF of a jammer-free $(B-I) \times U$ MIMO system as described in Prop. 4.

Note that the results in Prop. 3 and Prop. 4 are independent of the distribution of the jammer's transmit signal \mathbf{w} (and, in particular, of its power). In contrast to finite-resolution MIMO communication systems, *infinite-resolution* systems are thus resilient to arbitrarily strong single-antenna jammers. It is instructive to compare the lower bound $\underline{I}(\mathbf{H}, \mathbf{J})$ from Prop. 3 to the mutual information of a jammer-free $B \times U$ MIMO system when the input is $\mathbf{s} \sim \mathcal{CN}(\mathbf{0}, \mathbf{I}_U)$ distributed, which is

$$I_{\text{JF}}(\mathbf{H}) = \log |\mathbf{N}_0^{-1} \mathbf{H} \mathbf{H}^H + \mathbf{I}_B|. \quad (24)$$

In Fig. 3, we plot the CDFs of $\underline{I}(\mathbf{H}, \mathbf{J})$ and $I_{\text{JF}}(\mathbf{H})$ for the same system parameters as in Sec. IV-B. For the Rayleigh fading scenario in Fig. 3(a), we also plot the CDF of $I_{\text{JF}}(\tilde{\mathbf{H}})$, where $\tilde{\mathbf{H}}$ is as described in Prop. 4. The results show that, especially for Rayleigh fading (Fig. 3(a)), $I_{\text{JF}}(\mathbf{H})$ is only marginally lower than $\underline{I}(\mathbf{H}, \mathbf{J})$. Since the mutual information $I(\mathbf{y}; \mathbf{s})$ is lower-bounded by $I_{\text{JF}}(\mathbf{H})$, this implies that the achievable communication rates in the jammed system are not significantly lower than those in an equivalent jammer-free system—irrespective of the strength of the jammer signal.⁵ Note also that, as expected from Prop. 4, the CDF of $\underline{I}(\mathbf{H}, \mathbf{J})$ in Fig. 3(a) overlaps perfectly with the one of $I_{\text{JF}}(\tilde{\mathbf{H}})$.

APPENDIX B PROOFS

A. Proof of Thm. 1

We start by defining the sum of the receive interference and the noise, $\mathbf{d} \triangleq \mathbf{z} + \mathbf{n}$, so that $\mathbf{y} = \mathbf{r} + \mathbf{d}$ and $\mathbf{q} = \mathcal{Q}(\mathbf{y})$. Then

$$I(\mathbf{q}; \mathbf{s}) \leq I(\mathbf{q}; \mathbf{r}) \leq I(\mathbf{q}, \mathbf{d}; \mathbf{r}) \quad (25)$$

$$= \underbrace{I(\mathbf{d}; \mathbf{r})}_{=0} + I(\mathbf{q}; \mathbf{r} | \mathbf{d}) = H(\mathbf{q} | \mathbf{d}) - H(\mathbf{q} | \mathbf{d}, \mathbf{r}) \quad (26)$$

$$\leq \sum_{c \in \mathcal{C}} H(q_c | d_c) - H(\mathbf{q} | \mathbf{d}, \mathbf{r}) \quad (27)$$

$$= \sum_{c \in \mathcal{C}} \underbrace{(H(q_c | d_c) - H(q_c | d_c, r_c))}_{=I(q_c; r_c | d_c)} \quad (28)$$

where (25) follows from the data processing inequality [17]; where $I(\mathbf{d}; \mathbf{r}) = 0$ in (26) follows from the independence of \mathbf{d}

⁵In the case of LoS (Fig. 3(b)), the gap between the jammed system and the jammer-free system is larger than in Rayleigh fading because of the limited spatial diversity. However, also in this case, the lower bound on the mutual information is independent of the jammer power.

and \mathbf{r} ; where (27) follows since conditioning reduces entropy; and where (28) follows because $H(\mathbf{q} | \mathbf{d}, \mathbf{r})$ and the $H(q_c | d_c, r_c)$ are all equal to zero. The second argument in the minimum of (8) is due to the fact that the mutual information is also bounded by the capacity of an unquantized, jammer-free system. ■

B. Proof of Thm. 2

We start by defining $d_c \triangleq z_c + n_c$ and the random variable

$$f \triangleq \mathbb{1}\{Q_c(r_c + d_c) \neq Q_c(d_c)\} \quad (29)$$

$$= \mathbb{1}\{q_c \neq Q_c(d_c)\}. \quad (30)$$

We then have

$$I(q_c; r_c | d_c) = H(q_c | d_c) - \underbrace{H(q_c | d_c, r_c)}_{=0} \quad (31)$$

$$= H(q_c | d_c) + \underbrace{H(f | q_c, d_c)}_{=0} \quad (32)$$

$$= H(q_c, f | d_c) = H(f | d_c) + H(q_c | d_c, f) \quad (33)$$

$$\leq H(f) + H(q_c | d_c, f) \quad (34)$$

where (31) follows from $q_c = Q_c(d_c + r_c)$; (32) follows because f is a function of q_c and d_c (see (30)); (33) uses the chain rule of entropy twice; and (34) follows because conditioning reduces entropy. The second term in (34) can now be bounded as

$$H(q_c | d_c, f) = \mathbb{P}(f = 0) \cdot \underbrace{H(q_c | d_c, f = 0)}_{=0} + \mathbb{P}(f = 1) \cdot H(q_c | d_c, f = 1) \quad (35)$$

$$\leq \mathbb{P}(f = 1) \log(M - 1) \quad (36)$$

where (35) follows because, conditional on $f = 0$, the quantizer output q_c is a deterministic function of d_c ; and where (36) follows since the conditional entropy of q_c is bounded by the logarithm of the alphabet cardinality minus one (conditional on $f = 1$, the alphabet value $Q(d_c)$ has probability zero).

Let $\Gamma = \{\gamma_1, \dots, \gamma_{M-1}\}$ denote the set of boundaries between the quantization levels of Q_c . Then we define the distance between $x \in \mathbb{R}$ and the nearest quantization boundary as

$$\Delta_\Gamma(x) = \min_{\gamma \in \Gamma} |x - \gamma|, \quad (37)$$

which allows us to bound the probability $\mathbb{P}(f = 1 | d_c = x)$:

$$\mathbb{P}(f = 1 | d_c = x) \leq \mathbb{P}(|r_c| \geq \Delta_\Gamma(x)) \leq \min\left\{1, \frac{R_c}{\Delta_\Gamma^2(x)}\right\}, \quad (38)$$

where we have used the Markov bound in the second step. Using the law of total probability, we then bound $\mathbb{P}(f = 1)$ as

$$\mathbb{P}(f = 1) = \int_{\mathbb{R}} \mathbb{P}(f = 1 | d_c = x) p_{d_c}(x) dx \quad (39)$$

$$\leq \max_{\substack{\Gamma \subset \mathbb{R} \\ |\Gamma| = M-1}} \int_{\mathbb{R}} \min\left\{\frac{R_c}{\Delta_\Gamma^2(x)}, 1\right\} p_{d_c}(x) dx \quad (40)$$

$$= \max_{\Gamma} \int_{\mathbb{R}} \max_{\gamma \in \Gamma} g(x - \gamma) p_{d_c}(x) dx, \quad (41)$$

where p_{d_c} is the density of $d_c \sim \mathcal{N}(0, (Z_c + N_0)/2)$ and

$$g(x) \triangleq \min\left\{1, \frac{R_c}{|x|^2}\right\}. \quad (42)$$

Here, (40) follows from (38) and by maximizing over all possible boundary sets Γ . Both g and p_{d_c} are positive even Lipschitz continuous functions that are non-increasing on $[0, \infty)$.

The rest of the proof, which is somewhat technical, serves to show that (41), and hence $\mathbb{P}(f = 1)$, is upper bounded by

$$\int_{\mathbb{R}} g\left(\frac{x}{M-1}\right) p_{d_c}(x) dx \quad (43)$$

$$= \int_{x \in [-(M-1)\sqrt{R_c}, (M-1)\sqrt{R_c}]} p_{d_c}(x) dx + \int_{x \notin [-(M-1)\sqrt{R_c}, (M-1)\sqrt{R_c}]} \frac{R_c(M-1)^2}{x^2} p_{d_c}(x) dx \quad (44)$$

$$= \operatorname{erf}\left(\frac{(M-1)\sqrt{R_c}}{\sqrt{2(Z_c + N_0)}}\right) + \sqrt{\frac{2R_c}{\pi(Z_c + N_0)}}(M-1) \exp\left(-\frac{(M-1)^2 \operatorname{SINR}_c}{2}\right) - (M-1)^2 \frac{R_c}{Z_c + N_0} \operatorname{erfc}\left(\frac{(M-1)\sqrt{R_c}}{\sqrt{2(Z_c + N_0)}}\right) \quad (45)$$

$$= \bar{f}(M, \operatorname{SINR}_c), \quad (46)$$

where the last step follows since $\operatorname{SINR}_c = R_c/(Z_c + N_0)$. By then combining (34), (36), and (46), we obtain

$$I(q_c; r_c | d_c) \leq H(f) + H(q_c | d_c, f) \quad (47)$$

$$\leq H(f) + \mathbb{P}(f = 1) \log(M-1) \quad (48)$$

$$\leq H_b(\mathbb{P}(f = 1)) + \mathbb{P}(f = 1) \log(M-1) \quad (49)$$

$$\leq \bar{H}_b(\bar{f}(M, \operatorname{SINR}_c)) + \bar{f}(M, \operatorname{SINR}_c) \log(M-1). \quad (50)$$

and the theorem follows.

To fill the gap and show that (43) bounds (41) (see also Fig. 4), we write (41) as the limit of a sequence of integrals over the product of piecewise constant functions $g_n \approx g$ and $p_n \approx p_{d_c}$. Specifically, for $n = 1, 2, \dots$ and $\ell \in \mathbb{Z}$ we define the intervals

$$R_n(\ell) \triangleq [2^{-n}\ell, 2^{-n}\ell + 2^{-n}) \quad (51)$$

and the functions

$$\phi_n(x) \triangleq \lceil 2^n x \rceil, \quad (52)$$

$$g_n(x) \triangleq \sum_{\ell \in \mathbb{Z}} \left(\inf_{R_n(\ell)} g \right) \mathbb{1}\{x \in R_n(\ell)\}, \quad (53)$$

$$p_n(x) \triangleq \sum_{\ell \in \mathbb{Z}} \left(\inf_{R_n(\ell)} p_{d_c} \right) \mathbb{1}\{x \in R_n(\ell)\}. \quad (54)$$

For all $x, a \in \mathbb{R}$, it holds that

$$g(x-a) = \lim_{n \rightarrow \infty} g_n(x - 2^{-n}\phi_n(a)), \quad (55)$$

since, for $n = 1, 2, \dots$, we have

$$\begin{aligned} & |g_n(x - 2^{-n}\phi_n(a)) - g(x-a)| \\ & \leq |g_n(x - 2^{-n}\phi_n(a)) - g(x - 2^{-n}\phi_n(a))| \\ & \quad + |g(x - 2^{-n}\phi_n(a)) - g(x-a)| \end{aligned} \quad (56)$$

$$< L2^{-n} + |g(x - 2^{-n}\phi_n(a)) - g(x-a)| \quad (57)$$

$$< 2L2^{-n}, \quad (58)$$

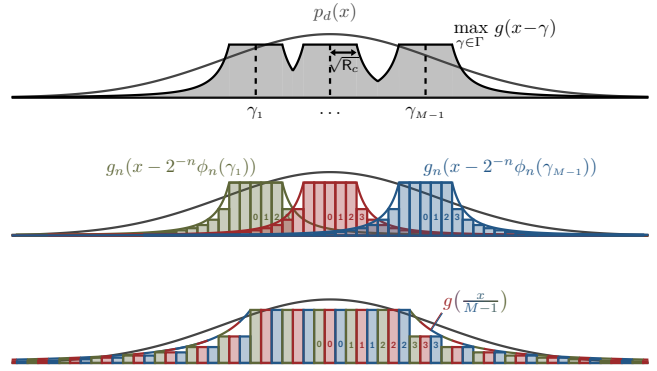


Fig. 4. Top: Illustration of the integral in (41) for an arbitrary boundary set Γ . Middle: Illustration of the discretization $g_n \approx g$ (for finite n) used in (60). The discretization $p_n \approx p_{d_c}$ is not shown to preserve figure legibility. Bottom: For any n and Γ , the inner product of p_{d_c} (or its discretized version p_n) with $\max_{\gamma \in \Gamma} g_n(x - 2^{-n}\phi_n(\gamma))$ is upper bounded by rearranging the piecewise constant segments of the $M-1$ translations of g_n as shown in the bottom figure. The rearranged segments converge to $g(x/(M-1))$ as $n \rightarrow \infty$.

where L is the Lipschitz constant of g . Here, (56) follows from the triangle inequality; (57) follows from the L -Lipschitz continuity of g and the fact that the length of the interval $R_n(\ell)$ in (53) is bounded by 2^{-n} ; and (58) follows from the L -Lipschitz continuity of g and the fact that $|2^{-n}\phi_n(a) - a| < 2^{-n}$.

An analogous line of reasoning shows that, for all $x \in \mathbb{R}$,

$$p_{d_c}(x) = \lim_{n \rightarrow \infty} p_n(x). \quad (59)$$

Plugging these limits into (41), and using the product law for limits and the fact that the maximum is a continuous function, gives (60); (61) can be shown by applying Lebesgue's dominated convergence theorem; and (63) follows (i) from the fact that $R_n(\ell) \cap R_n(\ell') = \emptyset$ for all n and all $\ell \neq \ell'$, and (ii) from the fact that $\operatorname{image}(\phi_n) \subset \mathbb{Z}$. The step to (64) follows by relaxing the maximization problem over boundary sets Γ to an optimization over surjections $\pi_k : \mathbb{Z} \rightarrow \mathbb{Z}$, $k \in [M-1]$. We then define Π as the set of $(M-1)$ -tuples $\pi = (\pi_1, \dots, \pi_{M-1})$ of surjections π_k for which, for every two surjections $\pi_k, \pi_{k'}$ out of π , it holds that $\operatorname{image}(\pi_{k'}) \cap \operatorname{image}(\pi_k) = \emptyset$. Since both g and p_d are positive, the maximum in (64) can be attained by an $(M-1)$ -tuple of surjections that is contained in Π (overlapping sections do not help, see Fig. 4), which gives (65). For such non-overlapping surjections, we have equality between (65) and (66); the step to (67) follows from the monotone convergence theorem. Since g and p_{d_c} are non-negative even functions that are non-increasing on $[0, \infty)$, we can deduce that optimal surjections $\hat{\pi} = (\hat{\pi}_1, \dots, \hat{\pi}_{M-1})$ are given by

$$\hat{\pi}_k(\ell) = k - 1 + \ell(M-1), \quad k = 1, \dots, M-1.$$

Inserting these into (67) gives (68). The step to (69) is obtained by interpreting $\hat{\pi}$ as a bijection from $[M-1] \times \mathbb{Z}$ to \mathbb{Z} , where (68) sums over the domain of $\hat{\pi}$ and (69) sums over the image of $\hat{\pi}$. (70) follows from the fact that $\sum_{\ell} \mathbb{1}\{x \in R_n(\ell)\} = \sum_{\ell} \sum_{\ell'} \mathbb{1}\{x \in R_n(\ell)\} \mathbb{1}\{x \in R_n(\ell')\}$. In (71), we use that $\lceil \ell/(M-1) \rceil$ stays constant for $M-1$ consecutive values of ℓ . Finally, (72) follows by taking the limit inside the integral (which is warranted by Lebesgue's dominated convergence theorem) and using (55) and (59). This concludes the proof. ■

$$\max_{\Gamma} \int_{\mathbb{R}} \max_{\gamma \in \Gamma} g(x - \gamma) p_{d_c}(x) dx = \max_{\Gamma} \int_{\mathbb{R}} \lim_{n \rightarrow \infty} \max_{\gamma \in \Gamma} g_n(x - 2^{-n} \phi_n(\gamma)) p_n(x) dx \quad (60)$$

$$= \lim_{n \rightarrow \infty} \max_{\Gamma} \int_{\mathbb{R}} \max_{\gamma \in \Gamma} g_n(x - 2^{-n} \phi_n(\gamma)) p_n(x) dx \quad (61)$$

$$= \lim_{n \rightarrow \infty} \max_{\Gamma} \int_{\mathbb{R}} \max_{\gamma \in \Gamma} \sum_{\ell \in \mathbb{Z}} \sum_{\ell' \in \mathbb{Z}} \left(\inf_{R_n(\ell)} g \right) \left(\inf_{R_n(\ell')} p_{d_c} \right) \mathbb{1}\{x - 2^{-n} \phi_n(\gamma) \in R_n(\ell)\} \mathbb{1}\{x \in R_n(\ell')\} dx \quad (62)$$

$$= \lim_{n \rightarrow \infty} \max_{\Gamma} \int_{\mathbb{R}} \max_{\gamma \in \Gamma} \sum_{\ell \in \mathbb{Z}} \left(\inf_{R_n(\ell)} g \right) \left(\inf_{R_n(\ell + \phi_n(\gamma))} p_{d_c} \right) \mathbb{1}\{x \in R_n(\ell + \phi_n(\gamma))\} dx, \quad (63)$$

$$\leq \lim_{n \rightarrow \infty} \max_{\pi_1, \dots, \pi_{M-1}} \int_{\mathbb{R}} \max_{k \in [M-1]} \sum_{\ell \in \mathbb{Z}} \left(\inf_{R_n(\ell)} g \right) \left(\inf_{R_n(\pi_k(\ell))} p_{d_c} \right) \mathbb{1}\{x \in R_n(\pi_k(\ell))\} dx \quad (64)$$

$$= \lim_{n \rightarrow \infty} \max_{\pi \in \Pi} \int_{\mathbb{R}} \max_{k \in [M-1]} \sum_{\ell \in \mathbb{Z}} \left(\inf_{R_n(\ell)} g \right) \left(\inf_{R_n(\pi_k(\ell))} p_{d_c} \right) \mathbb{1}\{x \in R_n(\pi_k(\ell))\} dx \quad (65)$$

$$= \lim_{n \rightarrow \infty} \max_{\pi \in \Pi} \int_{\mathbb{R}} \sum_{k \in [M-1]} \sum_{\ell \in \mathbb{Z}} \left(\inf_{R_n(\ell)} g \right) \left(\inf_{R_n(\pi_k(\ell))} p_{d_c} \right) \mathbb{1}\{x \in R_n(\pi_k(\ell))\} dx \quad (66)$$

$$= \lim_{n \rightarrow \infty} \max_{\pi \in \Pi} \sum_{k \in [M-1]} \sum_{\ell \in \mathbb{Z}} \left(\inf_{R_n(\ell)} g \right) \left(\inf_{R_n(\pi_k(\ell))} p_{d_c} \right) \underbrace{\int_{\mathbb{R}} \mathbb{1}\{x \in R_n(\pi_k(\ell))\} dx}_{=2^{-n}} \quad (67)$$

$$= \lim_{n \rightarrow \infty} \int_{\mathbb{R}} \sum_{(k, \ell) \in [M-1] \times \mathbb{Z}} \left(\inf_{R_n(\ell)} g \right) \left(\inf_{R_n(k-1 + \ell(M-1))} p_{d_c} \right) \mathbb{1}\{x \in R_n(k-1 + \ell(M-1))\} dx \quad (68)$$

$$= \lim_{n \rightarrow \infty} \int_{\mathbb{R}} \sum_{\ell' \in \mathbb{Z}} \left(\inf_{R_n(\lfloor \ell' / (M-1) \rfloor)} g \right) \left(\inf_{R_n(\ell')} p_{d_c} \right) \mathbb{1}\{x \in R_n(\ell')\} dx \quad (69)$$

$$= \lim_{n \rightarrow \infty} \int_{\mathbb{R}} \sum_{\ell \in \mathbb{Z}} \left(\inf_{R_n(\lfloor \ell / (M-1) \rfloor)} g \right) \mathbb{1}\{x \in R_n(\ell)\} \sum_{\ell' \in \mathbb{Z}} \left(\inf_{R_n(\ell')} p_{d_c} \right) \mathbb{1}\{x \in R_n(\ell')\} dx \quad (70)$$

$$= \lim_{n \rightarrow \infty} \int_{\mathbb{R}} \sum_{\ell \in \mathbb{Z}} \left(\inf_{R_n(\ell)} g \right) \mathbb{1}\{x / (M-1) \in R_n(\ell)\} \sum_{\ell' \in \mathbb{Z}} \left(\inf_{R_n(\ell')} p_{d_c} \right) \mathbb{1}\{x \in R_n(\ell')\} dx \quad (71)$$

$$= \int_{\mathbb{R}} g\left(\frac{x}{M-1}\right) p_{d_c}(x) dx, \quad (72)$$

C. Proof of Thm. 3

We first show that the function $\bar{I}(M, \rho, \mathbf{H}, \mathbf{J})$ in (16) is an increasing function of SINR_c . This follows since the function $x \mapsto \min\{\log M, \bar{H}_b(x) + x \log(M-1)\}$ is increasing, and since the function $\bar{f}(M, \text{SINR}_c)$ in (10) is increasing in SINR_c (this can be seen by taking the derivative with respect to SINR_c and observing that it is non-negative). Thus, the result follows by proving that $\bar{\text{SINR}}_c$ from (16) is an upper bound to SINR_c from Thm. 2 for suitable marginal distributions of the jammer interference z_c , the noise n_c , and the legitimate signal r_c :

Consider an index $c \in \{(b, \tau), (b, i)\}$. Since the entries s_u of \mathbf{s} are uncorrelated and satisfy $\mathbb{E}[|s_u|^2] \leq 1$, it follows⁶

$$\mathbb{E}[|r_c|^2] \leq \mathbb{E}[|r_{(b, \tau)} + ir_{(b, i)}|^2] \quad (73)$$

$$= \mathbb{E}[|\mathbf{h}_{(b)}^T \mathbf{s}|^2] = \mathbf{h}_{(b)}^T \mathbb{E}[\mathbf{s} \mathbf{s}^H] \mathbf{h}_{(b)}^* \quad (74)$$

$$= \mathbf{h}_{(b)}^T \text{diag}(\mathbb{E}[|s_1|^2], \dots, \mathbb{E}[|s_U|^2]) \mathbf{h}_{(b)}^* \quad (75)$$

$$\leq \|\mathbf{h}_{(b)}\|_2^2. \quad (76)$$

⁶If $\mathbf{s} \sim \mathcal{CN}(\mathbf{0}, \mathbf{I}_U)$, then $r_{(b, \tau)} + ir_{(b, i)} = \mathbf{h}_{(b)}^T \mathbf{s} \sim \mathcal{CN}(0, \|\mathbf{h}_{(b)}\|_2^2)$, so that $r_{(b, \tau)}$ and $r_{(b, i)}$ are $\mathcal{N}(0, \|\mathbf{h}_{(b)}\|_2^2/2)$ distributed. This implies Rem. 2.

Since $\mathbf{w} \sim \mathcal{CN}(\mathbf{0}, \rho \mathbf{I}_I)$, the distribution of $z_{(b, \tau)} + iz_{(b, i)}$ is

$$z_{(b, \tau)} + iz_{(b, i)} = \mathbf{j}_{(b)} \mathbf{w} \sim \mathcal{CN}(\mathbf{0}, \rho \|\mathbf{j}_{(b)}\|_2^2), \quad (77)$$

meaning that both $z_{(b, \tau)}$ and $z_{(b, i)}$ are $\mathcal{N}(0, \rho \|\mathbf{j}_{(b)}\|_2^2/2)$ distributed. And since $\mathbf{n} \sim \mathcal{CN}(\mathbf{0}, N_0 \mathbf{I}_I)$, the distribution of both $n_{(b, \tau)}$ and $n_{(b, i)}$ is $\mathcal{N}(0, N_0/2)$. Hence, the conditions of Thm. 2 are fulfilled with a SINR that is bounded by

$$\text{SINR}_c \leq \frac{\|\mathbf{h}_{(b)}\|_2^2}{\rho \|\mathbf{j}_{(b)}\|_2^2/2 + N_0/2} = \bar{\text{SINR}}_c. \quad (78)$$

From this, the result follows. \blacksquare

D. Proof of Prop. 1

Since all rows $\mathbf{j}_{(b)}$ of \mathbf{J} are nonzero, we have $\bar{\text{SINR}}_c \xrightarrow{\rho \rightarrow \infty} 0$ for all $c \in \mathcal{C}$, see (16). The result now follows directly from Thm. 3, considering the fact that $\bar{f}(M, \text{SINR}_c) \xrightarrow{\text{SINR}_c \rightarrow 0} 0$ and that $\bar{H}_b(x) \xrightarrow{x \rightarrow 0} 0$. \blacksquare

E. Proof of Prop. 2

Since all terms of $\bar{I}(M, \rho, \mathbf{H}, \mathbf{J})$ in (14) depend on ρ and M and have the same structure, it suffices to consider the

conditions under which one of the terms tends to zero as $\rho \rightarrow \infty$. Let $M = M(\rho)$ be a function of the jammer power ρ , and recall that $\overline{\text{SINR}}_c = \overline{\text{SINR}}_c(\rho)$ is a function of ρ , too (see (16)). By dropping the minimum from (11), the c -th term of the bound in (14) can then be upper-bounded with

$$T_c(\rho) \triangleq \bar{H}_b(\bar{f}(\rho)) + \bar{f}(\rho) \log(M(\rho) - 1), \quad (79)$$

where $\bar{f}(\rho) \triangleq \bar{f}(M(\rho), \overline{\text{SINR}}_c(\rho))$ is defined on $\rho \in [0, \infty)$. Both terms in (79) are nonnegative, so that $T_c(\rho)$ stays bounded away from zero if and only if either of its terms stays bounded away from zero. The first term stays bounded away from zero if and only if $\bar{f}(\rho)$ does; the second term stays bounded away from zero if and only if $\bar{f}(\rho) \log(M(\rho) - 1)$ does. Since $M(\rho) \geq 2$ holds, $\bar{f}(\rho) \log(M(\rho) - 1) \rightarrow 0$ implies $\bar{f}(\rho) \rightarrow 0$, so we only need to consider the conditions under which $\bar{f}(\rho) \log(M(\rho) - 1)$ stays bounded away from zero as $\rho \rightarrow \infty$.

We start by providing the following bound on $\bar{f}(\rho)$, see (10):

$$0 \leq \bar{f}(\rho) \leq \operatorname{erf}\left(\frac{(M(\rho) - 1)\sqrt{\overline{\text{SINR}}_c(\rho)}}{\sqrt{2}}\right) + \sqrt{\frac{2}{\pi}}(M(\rho) - 1)\sqrt{\overline{\text{SINR}}_c(\rho)} \quad (80)$$

$$\leq 2\sqrt{\frac{2}{\pi}}(M(\rho) - 1)\sqrt{\overline{\text{SINR}}_c(\rho)} \quad (81)$$

$$= \bar{f}(M(\rho), \overline{\text{SINR}}_c(\rho)). \quad (82)$$

In (80) we have used that $\exp(-x) \leq 1$ and $\operatorname{erfc}(\sqrt{x}) \leq 0$ for $x \geq 0$; in (81), we have used that⁷ $\operatorname{erf}(x) \leq 2x/\sqrt{\pi}$ for $x \geq 0$. Equations (80)–(82) also imply Rem. 1. Since $\sqrt{8/\pi} \leq 2$, $M(\rho) - 1 \leq M(\rho)$, and $\overline{\text{SINR}}_c(\rho) \leq \frac{2\|\mathbf{h}_{(b)}\|_2^2}{\rho\|\mathbf{j}_{(b)}\|_2^2}$, it follows that

$$0 \leq \bar{f}(\rho) \log(M(\rho) - 1) \leq \frac{\sqrt{32}\|\mathbf{h}_{(b)}\|_2}{\|\mathbf{j}_{(b)}\|_2} \frac{M(\rho)}{\sqrt{\rho}} \log(M(\rho)). \quad (83)$$

For any $\epsilon > 0$, if $M(\rho) = \rho^{\frac{1}{2} - \epsilon}$, then the right-hand-side of (83) tends to zero as $\rho \rightarrow \infty$, which implies that $\bar{f}(\rho) \log(M(\rho) - 1)$ tends to zero as well.

It follows that $M \prec \sqrt{\rho}$ implies $\lim_{\rho \rightarrow \infty} \bar{I}(M, \rho, \mathbf{H}, \mathbf{J}) = 0$ and, logically equivalently, that $\lim_{\rho \rightarrow \infty} \bar{I}(M, \rho, \mathbf{H}, \mathbf{J}) > 0$ implies $M \succeq \sqrt{\rho}$. ■

F. Proof of Prop. 3

We have

$$I(\mathbf{y}; \mathbf{s}) \geq I(\mathbf{U}_\perp^H \mathbf{y}; \mathbf{s}) = h(\mathbf{U}_\perp^H \mathbf{y}) - h(\mathbf{U}_\perp^H \mathbf{y} | \mathbf{s}) \quad (84)$$

$$= \log |\pi e \mathbf{U}_\perp^H (\mathbf{H}\mathbf{H}^H + N_0 \mathbf{I}_B) \mathbf{U}_\perp| - \log |\pi e N_0 \mathbf{I}_{B-I}| \quad (85)$$

$$= \log |N_0^{-1} \mathbf{U}_\perp^H \mathbf{H}\mathbf{H}^H \mathbf{U}_\perp + \mathbf{I}_{B-I}|, \quad (86)$$

where (84) follows from the data-processing inequality; and (85) follows since $\mathbf{U}_\perp \mathbf{y} \sim \mathcal{CN}(\mathbf{0}, \mathbf{U}_\perp^H (\mathbf{H}\mathbf{H}^H + N_0 \mathbf{I}_B) \mathbf{U}_\perp)$ (because $\mathbf{U}_\perp^H \mathbf{J} = \mathbf{0}$), since, conditional on \mathbf{s} , the vector $\mathbf{U}_\perp \mathbf{y}$ is circularly-symmetric complex Gaussian with covariance matrix $N_0 \mathbf{U}_\perp \mathbf{U}_\perp^H = N_0 \mathbf{I}_{B-I}$, and since the differential entropy of a complex Gaussian with covariance matrix Σ is $\log |\pi e \Sigma|$. ■

⁷This follows by $\operatorname{erf}(x) = \frac{2}{\sqrt{\pi}} \int_0^x e^{-t^2} dt \leq \frac{2}{\sqrt{\pi}} \int_0^x 1 dt = \frac{2x}{\sqrt{\pi}}$ for $x \geq 0$.

G. Proof of Prop. 4

We have

$$\mathbf{U}_\perp^H \mathbf{y} = \underbrace{\mathbf{U}_\perp^H \mathbf{H} \mathbf{s}}_{\triangleq \tilde{\mathbf{H}}} + \underbrace{\mathbf{U}_\perp^H \mathbf{J} \mathbf{w}}_{=0} + \underbrace{\mathbf{U}_\perp^H \mathbf{n}}_{\triangleq \tilde{\mathbf{n}}} = \tilde{\mathbf{H}} \mathbf{s} + \tilde{\mathbf{n}}. \quad (87)$$

Since $\mathbf{H} \stackrel{\text{i.i.d.}}{\sim} \mathcal{CN}(0, 1)$ and the rows of \mathbf{U}_\perp^H are orthonormal, it follows that $\tilde{\mathbf{H}} \stackrel{\text{i.i.d.}}{\sim} \mathcal{CN}(0, 1)$. The orthonormality of the rows of \mathbf{U}_\perp^H as well as the fact that $\mathbf{n} \sim \mathcal{CN}(\mathbf{0}, N_0 \mathbf{I}_B)$ imply $\tilde{\mathbf{n}} \sim \mathcal{CN}(\mathbf{0}, N_0 \mathbf{I}_{B-I})$. This concludes the proof. ■

REFERENCES

- [1] H. Pirayesh and H. Zeng, "Jamming attacks and anti-jamming strategies in wireless networks: A comprehensive survey," *IEEE Commun. Surveys Tuts.*, vol. 9, no. 2, pp. 767–809, 2022.
- [2] Y. Léost, M. Abdi, R. Richter, and M. Jeschke, "Interference rejection combining in LTE networks?" *Bell Labs Tech. J.*, vol. 17, no. 1, pp. 25–50, Jun. 2012.
- [3] G. Marti and C. Studer, "Universal MIMO jammer mitigation via secret temporal subspace embeddings," in *Proc. Asilomar Conf. Signals, Syst., Comput.*, Oct. 2023, pp. 1–8.
- [4] C. Mollén, J. Choi, E. G. Larsson, and R. W. Heath Jr., "Uplink performance of wideband massive MIMO with one-bit ADCs," *IEEE Trans. Wireless Commun.*, vol. 16, no. 1, pp. 87–100, Jan. 2017.
- [5] S. Jacobsson, G. Durisi, M. Coldrey, U. Gustavsson, and C. Studer, "Throughput analysis of massive MIMO uplink with low-resolution ADCs," *IEEE Trans. Wireless Commun.*, vol. 16, no. 6, pp. 4038–4051, Jun. 2017.
- [6] O. T. Demir and E. Bjornson, "The Bussgang decomposition of nonlinear systems: Basic theory and MIMO extensions [lecture notes]," *IEEE Signal Process. Mag.*, vol. 38, no. 1, pp. 131–136, 2020.
- [7] F. J. Block, "Performance of wideband digital receivers in jamming," in *Proc. IEEE Mil. Commun. Conf. (MILCOM)*, 2006, pp. 1–7.
- [8] T. T. Do, E. Björnsson, E. G. Larsson, and S. M. Razavizadeh, "Jamming-resistant receivers for the massive MIMO uplink," *IEEE Trans. Inf. Forensics Security*, vol. 13, no. 1, pp. 210–223, Jan. 2018.
- [9] Y. Li, C. Tao, G. Seco-Granados, A. Mezghani, A. L. Swindlehurst, and L. Liu, "Channel estimation and performance analysis of one-bit massive MIMO systems," *IEEE Trans. Signal Process.*, vol. 65, no. 15, pp. 4075–4089, Aug. 2017.
- [10] F. Bucheli, O. Castañeda, G. Marti, and C. Studer, "A jammer-mitigating 267 Mb/s 3.78 mm² 583 mW 32×8 multi-user MIMO receiver in 22FDX," in *Proc. IEEE Int. Symp. VLSI Technol. Circuits*.
- [11] Z. Lu, J. Nie, J. Li, and G. Ou, "Effect of ADC non-ideal characteristics on GNSS antenna array anti-jamming," in *Int. Conf. Comput. Sci. Netw. Technol. (ICCSNT)*, 2016, pp. 512–516.
- [12] H. Pirzadeh, G. Seco-Granados, and A. L. Swindlehurst, "Mitigation of jamming attack in massive MIMO with one-bit FBB sigma-delta ADCs," in *Asilomar Conf. Signals, Syst., Comput.*, 2019, pp. 1700–1704.
- [13] G. Marti, O. Castañeda, S. Jacobsson, G. Durisi, T. Goldstein, and C. Studer, "Hybrid jammer mitigation for all-digital mmWave massive MU-MIMO," in *Proc. Asilomar Conf. Signals, Syst., Comput.*, Nov. 2021, pp. 93–99.
- [14] G. Marti, O. Castañeda, and C. Studer, "Jammer mitigation via beam-slicing for low-resolution mmWave massive MU-MIMO," *IEEE Open J. Circuits Syst.*, vol. 2, pp. 820–832, Dec. 2021.
- [15] W. Jiang, K. Huang, M. Yi, Y. Chen, and L. Jin, "RIS-based reconfigurable antenna for anti-jamming communications with bit-limited ADCs," in *Proc. IEEE Global Commun. Conf. (GLOBECOM)*, 2023, pp. 1433–1438.
- [16] M. A. Teeti, "One-bit window comparator based jamming detection in massive MIMO system," in *IEEE Veh. Technol. Conf. Spring (VTC-Spring)*, Apr. 2021, pp. 1–5.
- [17] T. M. Cover and J. A. Thomas, *Elements of Information Theory*. Wiley, 2006.